Modification of low and high defect kaolinite surfaces- Implications for kaolinite mineral processing

Ray L. Frost,•[1] Erzsébet Horváth, [2] Éva Makó,[3] and János Kristóf [4]

[1]*Inorganic Materials Research Program, School of Physical and Chemical Sciences, Queensland University of Technology, 2 George Street, GPO Box 2434, Brisbane Queensland 4001, Australia.*
[2]*Department of Environmental Engineering and Chemical Technology, University of Veszprem, H8201 Veszprem, P.O. Box 158, Hungary*
[3]*Department of Silicate and Materials Engineering, University of Veszprem, H-8201 Veszprem, P.O. Box 158, Hungary*
[4]*Department of Analytical Chemistry, University of Veszprem, H8201 Veszprem, P.O. Box 158, Hungary*

Published as

Frost, R.L., Horvath, E., Mako, E. & Kristof, J. Modification of low- and high-defect kaolinite surfaces: implications for kaolinite mineral processing. *Journal of Colloid and Interface Science,* 2004. 270(2): p. 337-46.

Abstract

A comparison is made of the mechanochemical activation of three low and one high defect kaolinites using a combination of X-ray diffraction, thermal analysis and DRIFT spectroscopy. The effect of mechanochemical alteration of the kaolinites is greatest for the low defect kaolinites. The effectiveness of the mechanochemical treatment is represented by the slope of the d(001)peakwidth-grinding time line. High defect kaolinites are not significantly altered by the grinding treatment. The effect of mechanochemical treatment on peakwidth was independent of the presence of quartz; the quartz acts as an additional grinding medium. The effectiveness of the mechanochemical treatment depends on the crystallinity of the kaolinite. Two processes are identified in the mechanochemical activation of the kaolinite: first the delamination of kaolinite appears to take place in the first hour of grinding and secondly a recombination process results in the reaggregation of the ground crystals. During this process proton hopping occurs and reaction to form water takes place. This water is then adsorbed and coordinated to surface active-sites created during mechanochemical treatment.

• Author to whom correspondence should be addressed (r.frost@qut.edu.au)

Introduction

The effect of grinding on the structure of kaolinite has been known for some time (1-4). The effect of grinding of soils containing kaolinite has also been elucidated (5). This effect influences the cation exchange capacity of the soil (6). In the 1960's the grinding of kaolinite was thought to produce a zeolite-like material. Two processes were identified: firstly the destruction of the kaolinite layers to create a new amorphous material and secondly the aggregation of the ground particles to produce an agglomerated material (7-10). It is probable that the mechanochemical modification of kaolinite results in the formation of xerogel type materials (11, 12). Such materials are no doubt on the nanometer scale and the effect of the dry grinding of kaolinite is a method of effectively synthesizing a nanomaterial. Dry grinding causes the kaolinite layers to fragment and results in the formation of spheroidal particles. (13, 14). It has been proposed that dry grinding removes the hydroxyl units from the kaolinite and results in the formation of new kaolinite surfaces (13, 14). Dry grinding of kaolinite with group I and II halides has been used to produce novel intercalates of kaolinite and it was proposed that dry grinding of the kaolinite resulted in an increased degree of intercalation (15-18). Dry grinding of minerals such as coals which contain kaolinite as an impurity has implications for the combustion of coals (19).

Numerous techniques have been used to study the effects of dry grinding. The most common technique is X-ray diffraction (20, 21). The problem is that dry grinding of the kaolinite eventually produces an amorphous material. This means that some other technique such as infrared spectroscopy is used to study changes in mineral structure (19, 22). Whilst infrared spectroscopy enables considerations of molecular structure, bulk properties might be ignored. Thermal analysis is often the technique of choice for the study of bulk phases (23, 24). TG and DTA measurements show that effects of dry grinding often alter dehydroxylation temperatures and influence higher temperature reactions. Such chemical changes have serious implications in the formation of ceramics (23, 24). Recent studies have shown the effect of mechanochemical activation of highly ordered kaolinite (25-28). Impurities such as quartz and their influence have not been taken into account in previous studies. In the case of the influence of the quartz, these studies have been undertaken by the authors. However, the effect of the presence of other minerals on the mechanochemical activation of kaolinite is not known (27). In this paper we report a comparison of the mechanochemical activation of four kaolinites and comment on implications for mineral processing of kaolinite by dry grinding.

Experimental

The kaolinite minerals

Kaolinites used in the experiments were high-grade natural kaolinites from sources in Hungary, Slovakia and Australia. Four kaolinites were used (a) the Szeg kaolinite from Hungary, (b) the Kiralyhegy kaolinite from Hungary (c), the Zettlitz kaolinite from Slovakia and (d) the Birdwood kaolinite from South Australia. The kaolinites used were selected (apart from the Kiralyhegy kaolinite) for this experiment because of their low quartz content and high purity.

The Kiralyhegy kaolinite is a very highly ordered kaolinite from Hungary. The material contains around 70% quartz. Its chemical composition as determined by classical methods in wt % is MgO, 0.51; CaO, 0.35; SiO_2, 81.59; Fe_2O_3, 0.07; K_2O, 0.05; Na_2O, 0.03; Al_2O_3, 12.1; TiO_2, 0.001; loss on ignition, 5.09. The specific surface area is 1.3 m^2/g. The chemical composition of the Szeg clay in wt % is MgO, 0.71; CaO, 0.53; SiO_2, 46.89; Fe_2O_3, 3.1; K_2O, 0.35; Na_2O, 0.16; Al_2O_3, 33.51; TiO_2, 0.06; loss on ignition, 14.33. The major mineral constituent is high-defect kaolinite (95 wt %) with a Hinckley index of around 0.4. The specific surface area is 33.5 m^2/g. Minor amounts of quartz (2 wt. %) and feldspar (3 wt %) are also present. The chemical composition of the Zettlitz (Sedlec) kaolin from Slovakia in wt. % as oxides, is MgO, 0.26; CaO, 0.54; SiO_2, 46.97; Fe_2O_3, 0.37; K_2O, 1.21; Al_2O_3, 36.32; TiO_2, 0.05; loss on ignition, 12.85. The major mineral component is low-defect kaolinite (92 wt. %) with a Hinckley index of around 0.7. Minor amounts of quartz (4 wt %) and illite (4 wt %) are also present. The specific surface area is 18.5 m^2/g. The kaolinite from Birdwood (Australia) is high-grade and is well crystallized with a Hinckley index > 1.3. It occurs as coarse, tightly packed crystal stacks in a matrix of fine-grained euhedral kaolinite crystals. The chemical composition in wt % as oxides is MgO, 0.07; CaO, 0.14; SiO_2, 46.97; Fe_2O_3, 0.17; K_2O, 0.21; Al_2O_3, 38.12; TiO_2, <0.01; loss on ignition, 15.27. The specific surface area is 16.2 m^2/g.

Milling procedure

A Fritsch pulverisette 5/2-type laboratory planetary mill was used to grind the kaolins. Samples were ground for 0, 1, 2, 3, 4 and 6 hours. All four kaolinites were ground under precisely the same conditions that have already been reported (25).

X-ray powder diffraction

The XRD analyses were carried out using a Philips PW 3020 vertical goniometer equipped with curved graphite-diffracted beam monochromator using CuKα radiation. Data collection and evaluation were performed with PC-APD 3.6 software. Profile fitting was applied to extract information concerning microstructure and structural defects of kaolinite and its alteration products.

Thermal analysis and surface area

Thermoanalytical investigations were carried out under dynamic heating conditions (10 °C/min) using a Netzsch (Germany) TG 209-type thermobalance in flowing argon atmosphere of 99.995% purity (Messer Griesheim, Hungary). Samples (10 mg) were heated in ceramic crucibles up to 1000°C.

The specific surface area of the samples was determined by the BET method from the adsorption of N_2 at 77.3 K with Micromeritics ASAP 2000 type equipment.

DRIFT spectroscopy

Diffuse Reflectance Fourier Transform Infrared (DRIFT) spectroscopic analyses were undertaken using a Bio-Rad FTS 60A spectrophotometer. 512 scans per spectrum were obtained at a resolution of 2 cm^{-1} with a mirror velocity of 0.3 cm/sec. Spectra were averaged to improve the signal to noise ratio. Approximately 3 weight % ground kaolinite was dispersed in 100 mg of oven dried spectroscopic grade KBr. Reflected radiation was collected at ~50% efficiency. Background KBr spectra were obtained and spectra ratioed to the background. The diffuse reflectance accessory used was designed exclusively by Bio-Rad for Bio-Rad FTS spectrometers. It is of the so-called “praying monk” design, and is mounted on a

kinematic baseplate. It includes two four-position sample slides and eight sample cups. The cup (3 mm deep, 6 mm in diameter) accommodates powder samples mixed with KBr.

Spectroscopic manipulation such as baseline adjustment, smoothing and normalization was performed using the Spectracalc software package GRAMS ® (Galactic Industries Corporation, NH, USA). Band component analysis was undertaken using the Jandel 'Peakfit' software package, which enabled the type of fitting function to be selected and allows specific parameters to be fixed or varied accordingly. Band fitting was done using a Lorentz-Gauss cross-product function with the minimum number of component bands used for the fitting process. The Gauss-Lorentz ratio was maintained at values greater than 0.7 and fitting was undertaken until reproducible results were obtained with squared correlations of R^2 greater than 0.995.

Results and Discussion

Surface Area

Grinding time [h]	specific surface area [m^2/g]			
	Birdwood	Szeg	Zettlitz	Királyhegy
0	16.2	33.5	18.5	1.3
1	33.2	39.5	34.4	5.9
2	43.1	43.3	42.8	-
3	44.7	47.0	43.3	8.2
4	-	-	47.0	
6	-	53.1	49.7	4.3
10	-	51.4	38.3	

Table 1 Specific surface area of selected kaolinites as a function of grinding time.

The investigation of specific surface areas shows that grinding consist of three steps in the case of samples from Szeg and Zettlitz. The produced new surface area is approximately proportional to the grinding time up to 2 hours (the Rittinger section). After 3, 4 and 6 hours of grinding, the degree of dispersion is characterised by the monotonous decrease of the rate of specific surface area increase as a function of grinding time (the aggregation section). After 10 hours of grinding the agglomeration causes a decrease the specific surface area value (the

agglomeration section). The specific surface area versus grinding time data of Birdwood and Kiralyhegy sample series can be separated into the Rittinger and the aggregation section. The Rittinger section belongs to the first 2 hours of grinding. After 3 hours of grinding the aggregation section appears.

XRD results

One means of following the structural degradation of kaolinite layers is to use X-ray diffraction. Such a technique is useful up to the point when the ground materials become X-ray amorphous. Thereafter, some other technique such as infrared spectroscopy becomes useful. The 001 reflections in the X-ray diffraction patterns for the four kaolinites studied in this work are shown in Figure 1. Figure 1a displays the XRD patterns of the untreated kaolinite; Figure 1b after 3 hours of grinding. The figures represent a progression of kaolinites in terms of crystallinity. Kiralyhegy kaolinite is very well ordered kaolinite with a high aspect ratio. The Hinckley index is 1.39. Birdwood kaolinite is also highly ordered with a Hinckely index of 1.35. This kaolinite also has a high aspect ratio but some of the plates appear to be eroded (29). The Zettlitz kaolinite has an index of 0.7. Szeg kaolinite is a high defect kaolinite with low aspect ratio and Hinckley index of 0.40. Figure 1 clearly shows a progression in peak widths of the d(001) peak with Hinckley index. Peak widths are in the order Kiralyhegy < Birdwood < Zettlitz < Szeg. The peaks may be deconvoluted into component peaks as is shown in Figure 1. For the Kiralyhegy kaolinite the two peaks are observed at 7.17 and 7.23 Å. The peak profile for the Birdwood kaolinite may be resolved into two peaks at 7.20 and 7.33 Å. Zettlitz kaolinite shows two peaks at 7.19 and 7.25Å. Szeg kaolinite appears to have a broad tail on the high Angstrom side and three peaks may be resolved at 7.23, 7.37 and 7.65 Å. Whether it is valid or not to undertake curve resolution of the d(001) peak is questionable. The observation of multiple peaks means that more than one phase is observed. What the component bands do illustrate is that there is a tail on the low angle (increased spacial distance) side of the peak. This means that there is a range of interspacial distances for each of the kaolinites, apart from Kiralyhegy kaolinite (30). This is particularly evident for the Szeg kaolinite. For this kaolinite, multiple peaks may be resolved for the d(001) spacing showing a range of interspatial distances.

What is evident is that the widths of the peaks for the low defect kaolinites increase with time of grinding. This variation is shown in Figure 2. The width of the peak is related to the crystallite size according to the Scherrer equation:

$$L = \frac{\lambda K}{\beta \cos \theta}$$

Where L is the mean crystallite dimension (Å) along a line normal to the reflecting plane, K is a constant close to unity, and β is the width of the reflection at half peak height

Plots of the d(001) peakwidth-grinding time data fit on single lines. This observation is comparable with the grinding of the Kiralyhegy kaolinite which contains some 70% quartz. The effectiveness of the mechanochemical treatment may be represented by the slope of the peakwidth of the d(001) peak with grinding time. The effectiveness is much greater for the Birdwood kaolinite than for any of the other kaolinites. Little if any effect of mechanochemical treatment regarding the peak width of the d(001) spacing is observed for the Szeg kaolinite. A decrease in the area of the d(001) peak is observed with mechanochemical grinding time. This means that the dislocation density of defects of the Szeg kaolinite is practically constant during the applied grinding experiments.

A number of conclusions may thus be drawn, as follows:

(a) The grinding activation causes an increase in peak width which is linear with grinding time for the kaolinites.

(b) Grinding activation increases the concentration of defect structures and reduces the crystallite size.

(c) There is apparently little effect on highly disordered kaolinite. Grinding activation does not increase the concentration of defect structures for the high defect kaolinite.

(d) The presence of quartz does not alter the slope of the line. For the Zettlitz kaolinite three experiments are shown: firstly mechanochemical activation without quartz (experiment 1); secondly mechanochemical activation with 50% quartz addition (experiment 2); thirdly with 75% quartz addition (experiment 3) (27).

(e) The grinding treatment delaminates kaolinite layers and the effect of quartz and other impurities may simply serve to keep the high surface area crystallites apart. This

delamination is evidenced by the loss of intensity of the d(001) peak with grinding time.

The results of the XRD study of the mechanochemically activated kaolinite have implications for mineral processing of kaolinite. The study shows that there is an optimum time for grinding. Too little grinding results in large particle sizes with low surface areas; there is an optimum grinding time for maximum surface area of the kaolinite; too much grinding results in a decrease in this optimum surface area.

Thermal Analysis

Mass loss (TG) and rate of mass loss (DTG) curves of the Kiralyhegy, Birdwood, Zettlitz and Szeg kaolinites are shown as a function of the time of grinding in Figures 3 (a to d). The amount of (dehydroxylation) water shows a gradual decrease with grinding time in all cases. At the same time, the amount of adsorbed water increases significantly (Figure 4a). Part of this adsorbed water may be the dehydroxylation water (lost as a result of mechanochemical activation) coordinated to the active centers (most likely aluminum ions) of the activated surface. The other sorbed water is adsorbed from the atmosphere. Figure 4b shows the decrease of the dehydroxylation (DTG) peak temperatures as a function of the grinding time. The Kiralyhegy clay shows a change almost an order of magnitude higher than the other minerals. The likely explanation of this phenomenon is the high quartz content of the mineral, since the quartz particles can act as micrometer-sized grinding bodies in intimate contact with clay particles. The significantly lower amount of adsorbed water in the case of the Kiralyhegy clay is also due to the high quartz (relatively low clay) content of the material.

DRIFT spectroscopy

One method for studying changes in the surface structure of kaolinites is to use DRIFT spectroscopy. (31-33) The kaolinite hydroxyl surface is mechanochemically activated upon grinding. Changes in the surface structure may be followed by changes in the hydroxyl stretching and deformation regions. The hydroxyl stretching region of kaolinite shows five features: (a) the in-phase inner surface hydroxyl stretching vibration normally observed around 3695 cm^{-1}, (b) the two out-of phase vibrations of the inner surface hydroxyl observed around 3668 and 3652 cm^{-1}, (c) the hydroxyl stretching vibration of the inner hydroxyl observed at 3620 cm^{-1}, (d) the transverse longitudinal optic vibration which is normally

Raman active and infrared inactive may be observed as a curve-resolved band at 3684 cm^{-1} in the DRIFT spectra of low defect kaolinites such as the Kiralyhegy and Birdwood kaolinites, (e) water OH stretching vibration of weakly hydrogen-bonded interstitial water observed as a band at 3595 cm^{-1} (34-39).

DRIFT spectra of the hydroxyl-stretching region of the four kaolinites mechanochemically activated for 0, 1, 2, 3, 6 hours are shown in Figures 5a, b, c, d, e, respectively. The figures show the DRIFT spectra of the kaolinite hydroxyl stretching region; the water OH stretching region is not shown as the bands are broad and of low intensity. The aforementioned features are readily observed in the spectra. Bands at 3695 and 3620 cm^{-1} are prominent. Two bands at 3668 and 3652 cm^{-1} are well resolved in the spectra of the low defect kaolinites. These bands for the Szeg kaolinite are not clearly defined and this part of the spectral region is more like a continuum. Such a feature is typical of a high defect kaolinite and also for a halloysite. In addition, for the Szeg kaolinite a band is observed at around 3600 cm^{-1} which is assigned to adsorbed water (40-42). The effect of mechanochemical activation of the kaolinites is to reduce layer stacking and crystallite size. There is a progressive decrease in the reduction rate of crystallite size of the kaolinites during grinding. This has significant effects upon DRIFT spectra of the hydroxyl stretching region.

Several significant spectral features are observed:

(a) Reduction in intensity of the band at 3695 cm^{-1} with grinding time
(b) Loss of intensity of the bands at around 3668 and 3652 cm^{-1} with grinding time
(c) The formation of a spectral continuum in this region as the low defect kaolinites are transformed into high defect kaolinites and
(d) The increase in a broad feature in the 3000 to 3550 cm^{-1} region attributed to adsorbed and coordinated water. (25, 26)

Effects of grinding on the kaolinite surface structure are observed by plotting changes in intensity of the hydroxyl-stretching bands with grinding time. Such dependencies are shown in Figures 6 a, b, c for the 3695, 3620 cm^{-1} and total water bands respectively. For the highly ordered kaolinites from Zettlitz and Kiralyhegy, the effect of mechanochemical treatment is most significant in the first hour of grinding. The effect then appears to level off and band intensity remains constant. The intensity of the 3695 cm^{-1} band for the Zettlitz kaolinite is reduced significantly after 2 hours of grinding. In contrast, the reduction in

intensity of the band due to the inner surface hydroxyl band is least for the Birdwood kaolinite. Reduction in intensity for the high defect kaolinite from Szeg appears linear. The question arises as to why there are differences in the intensity-grinding time relationships for the different kaolinites. Obviously there should be differences between low and high defect kaolinites as observed. All three low defect kaolinites have Hinckley indices in the 0.7 to 1.35 range, and thus the relationship is in some ways dependent on the Hinckley crystallinity number. Mechanochemical grinding breaks up the kaolinite layers. This apparently happens most acutely in the first hour of grinding. SEM images show that ground kaolinite particles agglomerate to take on a spherical shape. The fact that the results for the Birdwood kaolinite are different from that of the other kaolinites may be related to the difficulty of delaminating the various kaolinite layers (29).

The decrease in intensity of the band assigned to the inner hydroxyl observed at 3620 cm^{-1} appears to follow a similar pattern to that of the inner surface hydroxyls. A steady decrease in intensity is observed with the grinding time. The effect is less for the high defect kaolinite. While the intensities of the 3620 and 3695 cm^{-1} bands decrease, the intensity of the bands attributed to water OH stretching vibrations increases (Figure 6c). A number of conclusions may be made in the comparison of the mechanochemical activation of the kaolinites. First the low defect kaolinites from Zettlitz and Kiralyhegy have very high intensity in the bands attributed to the water OH stretching vibrations. Secondly the high defect kaolinite from Szeg does not show increased intensity of the OH stretching vibrations until after 3 hours of grinding. The results for the Birdwood kaolinite fits somewhere between the pattern of the low defect kaolinites and the high defect kaolinite.

The surface structural changes were followed by the use of DRIFT spectroscopy. The intensity of the hydroxyl stretching and deformation bands decreases with grinding time. At the same time the intensity of the water OH stretching bands increases in intensity. Significant change occurs in the first hour of grinding. This rate of change decreases with time. This suggests that two processes are involved namely the delamination of the kaolinite layers and secondly the reaggregation of the crystallites. Little if any effect is observed for the high defect kaolinite. The rate of decrease in intensity for the Birdwood kaolinite is less than that of the other two low defect kaolinites. This implies that the Birdwood kaolinite resembles a high defect kaolinite. This interpretation fits well with previous findings where it was suggested that the Birdwood kaolinite is composed of two kaolinites: a highly ordered

kaolinite and a disordered kaolinite which prevented the kaolinite form being completely intercalated. (29) If grinding removes the outer high defect kaolinite exposing the low defect kaolinite, this helps explain why the Birdwood kaolinite shows the greatest slope in the peakwidth grinding time plots and yet the rate of decrease of the intensity of the hydroxyl stretching band is less than that for the other low defect kaolinites.

The concept of proton migration through percussive grinding and their combination with hydroxyl units has been known for some time (43). The generally accepted concept of kaolinite dehydroxylation results from the interaction of two hydroxyl groups in a two step process to form a water molecule by proton transfer leaving a chemically bonded oxygen, as an oxide anion, in the lattice (43, 44). The reaction may be shown as follows:

$$=OH^- \leftrightarrow H^+ + =O^{2-} \qquad \text{and} \qquad H^+ + =OH^- \leftrightarrow =H_2O$$

These steps happen when mechanochemical activation of the kaolinite occurs. It is highly likely that point heating at specific sites during grinding is the cause of this dehydroxylation and this results in the increase in dehydroxylation with grinding time (45-48). These steps require proton delocalisation at specific hydroxyl sites. Such delocalisation may occur when the mechanochemical treatment of the kaolinite causes heating at the point of contact between two particles. For water to form, these protons must migrate to a second hydroxyl site. If two adjacent hydroxyls are involved in the two step process it will be homogenous; if, however, non adjacent hydroxyls are involved, such a process would require proton diffusion (sometimes referred to as proton hopping) and probably counteractive cation diffusion with the water molecules being produced at the outer surface. Where hydroxyls of different acidities are to be found, the homogenous process is more likely. It can be argued that kaolinites dehydroxylate by this homogenous process during mechanochemical activation.

Changes in the surface structure of kaolinites during mechanochemical activation may be also followed by using the hydroxyl deformation modes at 914 to 935 cm^{-1}. These two bands are attributed to the hydroxyl deformation of the inner and inner surface hydroxyls. In general, the two features at 935 and 914 cm^{-1} are observed for each of the kaolinites. Curve resolution for the low defect kaolinites enables an additional band at 925 cm^{-1} to be observed.

For the Szeg kaolinite a band is also observed at 877 cm^{-1}, ascribed to free or non-hydrogen bonded deformations. The variations in relative intensity of the 935 and 914 cm^{-1} bands are shown in Figure 7. In general the intensity of the 935 cm^{-1} band decreases with grinding time. The effect appears to be greater for the Zettlitz kaolinite. Concomitantly the relative intensity of the 914 cm^{-1} band increases.

The advantage of studying the hydroxyl deformation modes lies with the avoidance of the in-phase and out-of-phase behaviour and the overlap of water OH stretching bands. Consistent with the behaviour of the kaolinite OH stretching bands, the kaolinite hydroxyl deformation modes show a decrease in intensity with grinding time.

Implications for mineral processing

This research has implications for the processing of kaolinite. First the effects of dry grinding of kaolinite depend on the type of kaolinite and to some extent on its Hinckley Index. Secondly the optimum grinding time is dependent upon the initial water content. Thirdly the effectiveness of grinding depends upon the rate of change of crystallite size as measured by the change in peak width of the d(001) peak. Fourthly the rate of mechanochemical alteration may depend upon what impurities are present such as quartz. Such impurities act as a grinding medium and may be an advantage in that the particles serve to keep the surface active particles apart. In the case of the high defect kaolinite, the mechanochemical treatment decreases the content of the crystalline phase, but there is a parallel increase in defect density. This research shows that there is an optimum time for grinding kaolinite beyond which any further grinding will be of no benefit.

Acknowledgments

The financial and infra-structure support of the Queensland University of Technology Inorganic Materials Research Program of the School of Physical and Chemical Sciences is gratefully acknowledged.

REFERENCES

1. Gregg, S. J., Parker, T. W. and Stephens, M. J., *Clay Minerals Bull.* **2,** 34 (1953).
2. Gregg, S. J., Parker, T. W. and Stephens, M. J., *J. Appl. Chem. (London)* **4,** 666 (1954).

3. Gregg, S. J., Hill, K. J. and Parker, T. W., *J. Appl. Chem. (London)* **4,** 631 (1954).
4. Gregg, S. J., *Trans. Brit. Ceram. Soc.* **54,** 257 (1955).
5. Jackson, M. L. and Truog, E., *Soil Sci. Soc. Am. Proc.* **4,** 136 (1939).
6. Laws, W. D. and Page, J. B., *Soil Sci.* **62,** 319 (1946).
7. Takahashi, H., *Clays, Clay Minerals. Proc. Natl. Conf. Clays, Clay Minerals, 6th, Berkeley* 279 (1959).
8. Takahashi, H., *Bull. Chem. Soc. Japan* **32,** 252 (1959).
9. Takahashi, H., *Bull. Chem. Soc. Japan* **32,** 245 (1959).
10. Takahashi, H., *Bull. Chem. Soc. Japan* **32,** 235 (1959).
11. Juhasz, Z., *Acta Mineral.-Petrogr.* **24,** 121 (1980).
12. Juhasz, Z. and Wojnarovits, I., *CFI, Ceram. Forum Int./Ber. DKG* **61,** 131 (1984).
13. Gonzalez Garcia, F., Gonzalez Rodriguez, M., Gonzalez Vilchez, C. and Raigon Pichardo, M., *Bol. Soc. Esp. Ceram. Vidrio* **31,** 297 (1992).
14. Gonzalez Garcia, F., Ruiz Abrio, M. T. and Gonzalez Rodriguez, M., *Clay Miner.* **26,** 549 (1991).
15. Mackinnon, I. D. R., Uwins, P. J. R., Yago, A. J. E. and Thompson, J. G., *Clays Controlling Environ., Proc. Int. Clay Conf., 10th* 196 (1995).
16. Thompson, J. G., Uwins, P. J. R., Whittaker, A. K. and Mackinnon, I. D. R., *Clays Clay Miner.* **40,** 369 (1992).
17. Thompson, J. G., Gabbitas, N. and Uwins, P. J. R., *Clays Clay Miner.* **41,** 73 (1993).
18. Thompson, J. G., Gabbitas, N., Coyle, K., Uwins, P. J. R. and Mackinnon, I. D. R., *Clays Controlling Environ., Proc. Int. Clay Conf., 10th* 260 (1995).
19. Bandopadhyay, A. K., Bharathi, D. G., Maitra, S., Ansari, S. H., Mitra, S. and Sen, R., *Fuel Sci. Technol.* **16,** 115 (1997).
20. Dragsdorf, R. D., Kissinger, H. E. and Perkins, A. T., *Soil Sci.* **71,** 439 (1951).
21. Aglietti, E. F., Porto Lopez, J. M. and Pereira, E., *Int. J. Miner. Process.* **16,** 135 (1986).
22. Yariv, S. and Lapides, I., *Journal of Materials Synthesis and Processing* **8,** 223 (2000).
23. Sanchez-Soto, P. J., Justo, A. and Perez-Rodriguez, J. L., *J. Mater. Sci.* **29,** 1276 (1994).
24. Sanchez-Soto, P. J., Del Carmen Jimenez De Haro, M., Perez-Maqueda, L. A., Varona, I. and Perez-Rodriguez, J. L., *J. Am. Ceram. Soc.* **83,** 1649 (2000).
25. Groulx, R., Frost, R. and Tremblay, Y., in *Brit. UK Pat. Appl.*, (Mitel Corporation, Can.). Gb, 2001, p. 8 pp.
26. Frost, R. L., Kristof, J., Kloprogge, J. T. and Horvath, E., *Langmuir* **17,** 4067 (2001).
27. Mako, E., Frost, R. L., Kristof, J. and Horvath, E., *Journal of Colloid and Interface Science* **244,** 359 (2001).
28. Mako Eva, Kristof, J. and Zoltan, J. A., *Epitoanyag* **49,** 2 (1997).
29. Ruan, H. D., Frost, R. L., Kloprogge, J. T. and Duong, L., *Spectrochimica Acta, Part A: Molecular and Biomolecular Spectroscopy* **58,** 265 (2002).
30. Deluca, S. and Slaughter, M., *Am. Mineral.* **70,** 149 (1985).
31. Kloprogge, J. T. and Frost, R. L., *Neues Jahrb. Mineral., Monatsh.* 446 (2001).
32. Frost, R. L., Kristof, J., Mako, E. and Kloprogge, J. T., *Am. Mineral.* **85,** 1735 (2000).
33. Frost, R. L., Kristof, J., Mako, E. and Kloprogge, J. T., *Langmuir* **16,** 7421 (2000).
34. Frost, R. L. and Kloprogge, J. T., *J. Raman Spectrosc.* **31,** 415 (2000).
35. Frost, R. L., Kristof, J., Horvath, E. and Kloprogge, J. T., *Clay Minerals* **35,** 443 (2000).
36. Frost, R. L., Kristof, J., Horvath, E. and Kloprogge, J. T., *J. Colloid Interface Sci.* **214,** 380 (1999).
37. Frost, R. L., Kristof, J., Horvath, E. and Kloprogge, J. T., *J. Colloid Interface Sci.* **214,** 109 (1999).
38. Frost, R. L., *Clays Clay Miner.* **46,** 280 (1998).
39. Frost, R. L. and Gaast, S. J. V. D., *Clays and Clay Minerals* **45,** 68 (1997).
40. Frost, R. L., Kristof, J., Paroz, G. N., Tran, T. H. and Kloprogge, J. T., *J. Colloid Interface Sci.* **204,** 227 (1998).
41. Frost, R. L., Kristof, J., Paroz, G. N. and Kloprogge, J. T., *J. Colloid Interface Sci.* **208,** 478 (1998).
42. Frost, R. L. and Kristof, J., *Clays Clay Miner.* **45,** 551 (1997).
43. Miller, J. G. and Oulton, T. D., *Clays and Clay Minerals, Proceedings of the Conference* **18,** 313 (1970).
44. Yariv, S. and Shoval, S., *Clays and Clay Minerals, Proceedings of the Conference* **23,** 473 (1975).
45. Battalova, S. B. and Likerova, A. A., *Vestnik Akademii Nauk Kazakhskoi SSR* 54 (1985).
46. Brown, I. W. M., Mackenzie, K. J. D., Bowden, M. E. and Meinhold, R. H., *Journal of the American Ceramic Society* **68,** 298 (1985).
47. Guo, J., He, H., Wang, F., Wang, D., Zhang, H. and Hu, C., *Kuangwu Xuebao* **17,** 250 (1997).
48. Rocha, J., *Journal of Physical Chemistry B* **103,** 9801 (1999).

List of Figures

LIST OF TABLES

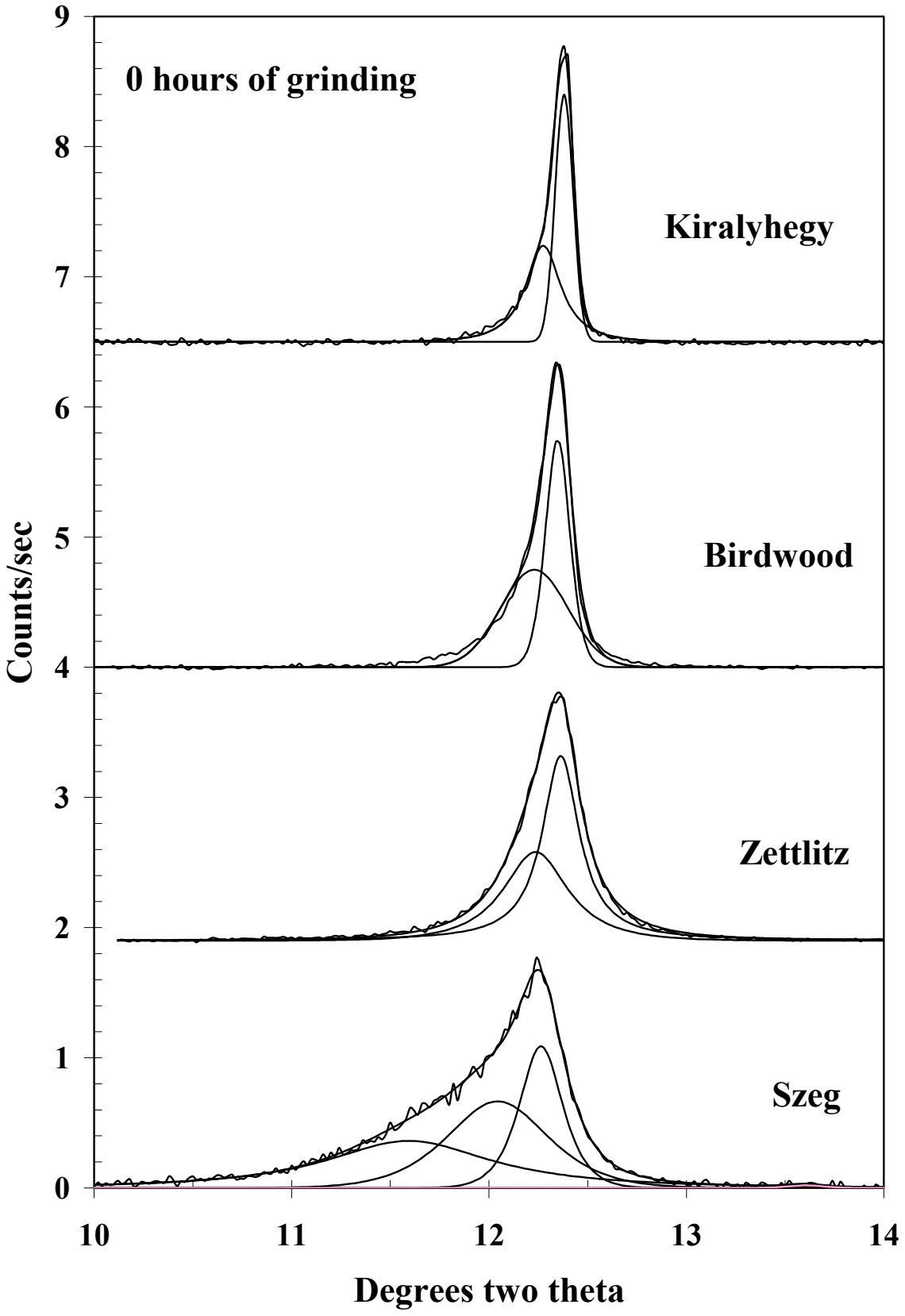
0 hours of grinding
Kiralyhegy
Birdwood
Zettlitz
Szeg
Counts/sec
Degrees two theta
0
1
2
3
4
5
6
7
8
9
10
11
12
13
14

Figure 1

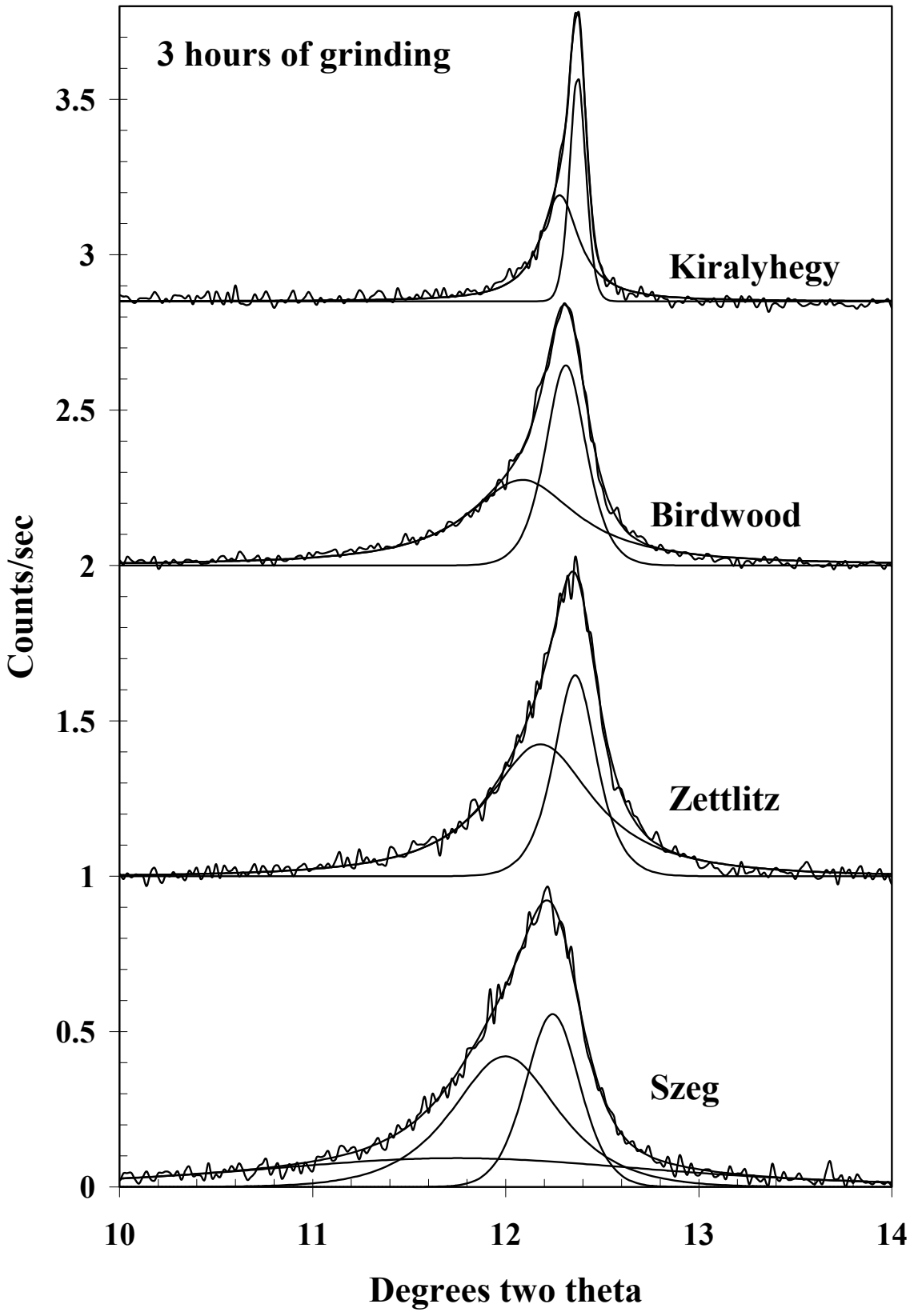
3 hours of grinding
Kiralyhegy
Birdwood
Zettlitz
Szeg
Counts/sec
Degrees two theta
0
0.5
1
1.5
2
2.5
3
3.5
10
11
12
13
14

Figure 1b

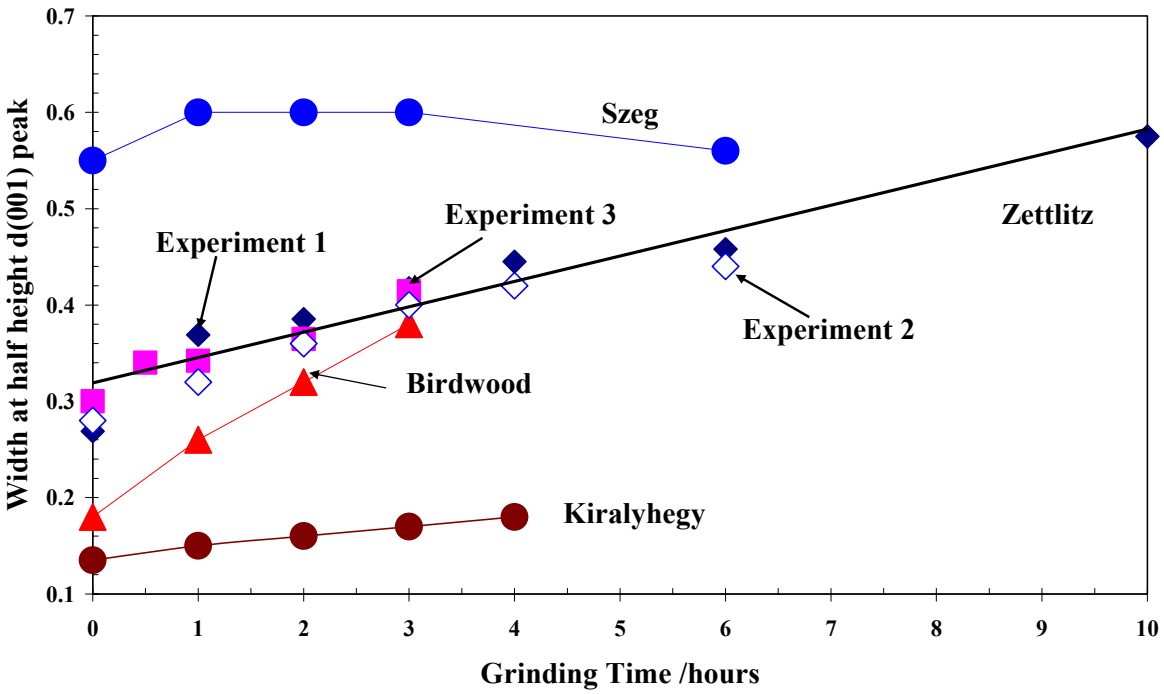
Width at half height d(001) peak
Grinding Time /hours
Szeg
Experiment 1
Experiment 3
Zettlitz
Experiment 2
Birdwood
Kiralyhegy
0.7
0.6
0.5
0.4
0.3
0.2
0.1
0
1
2
3
4
5
6
7
8
9
10

Figure 2

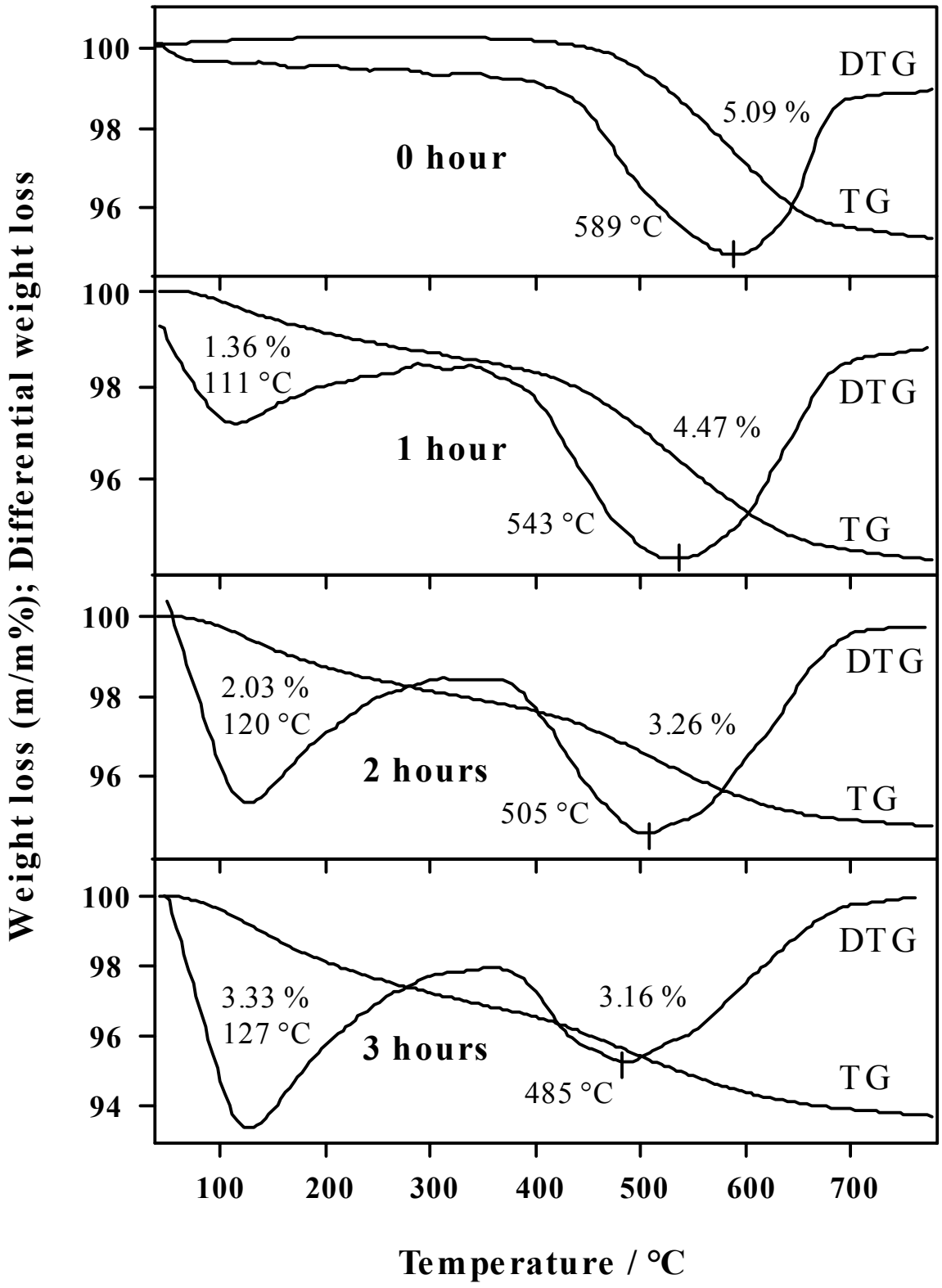

Figure 3a Frost et al Királyhegy

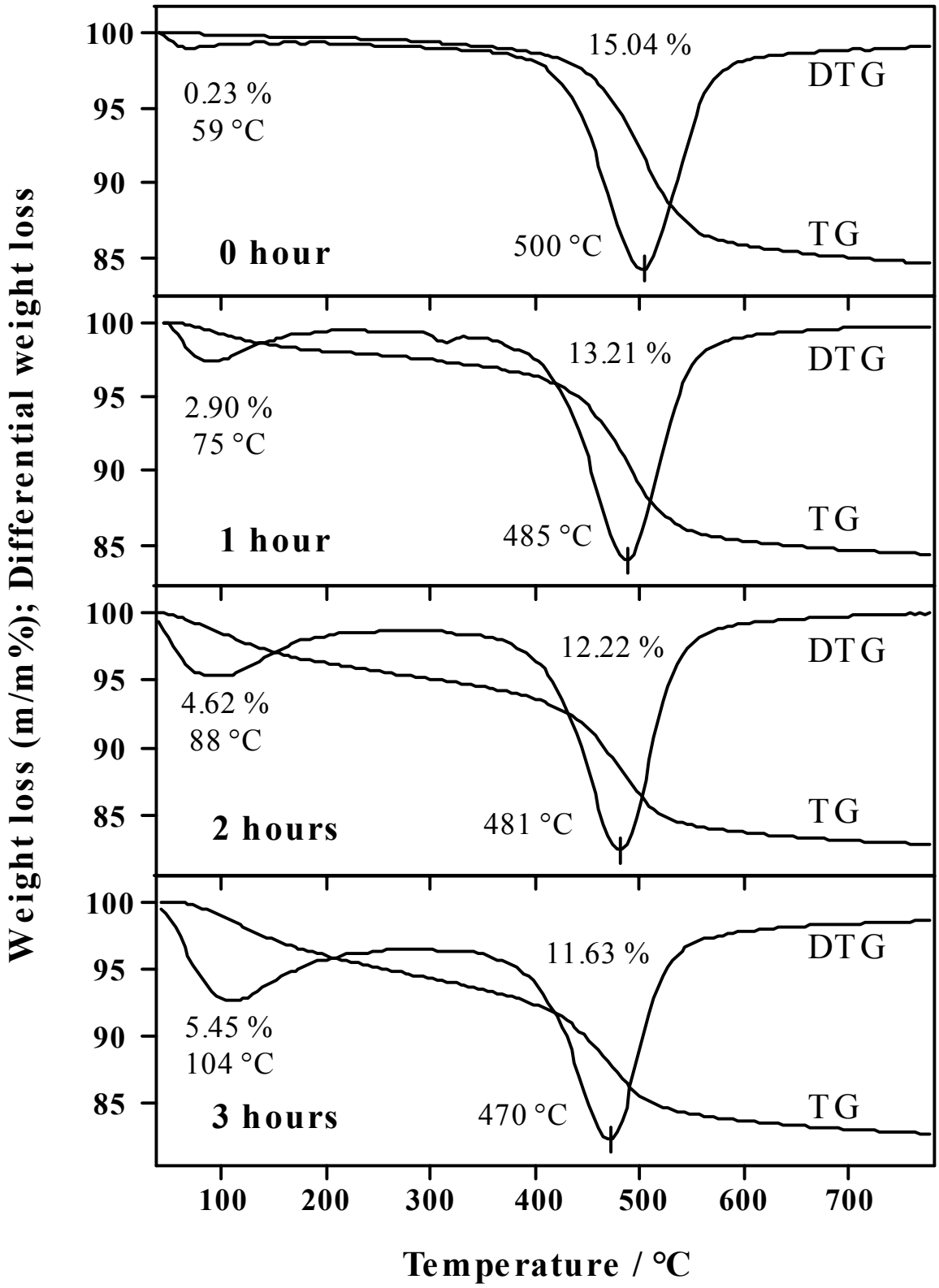

Figure 3b Frost et al.

Birdwood

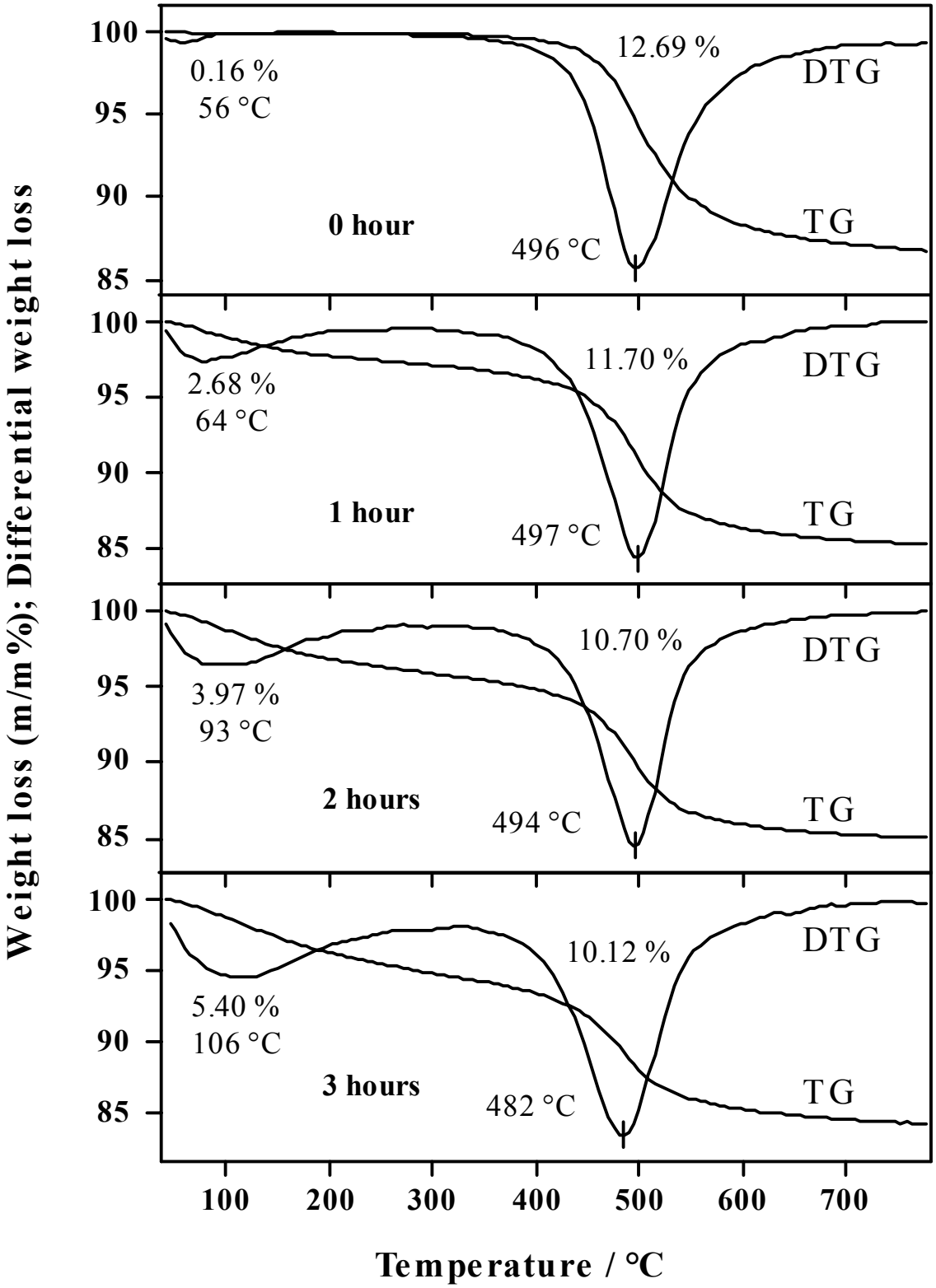

Figure 3c Frost et al.

Zettlitz

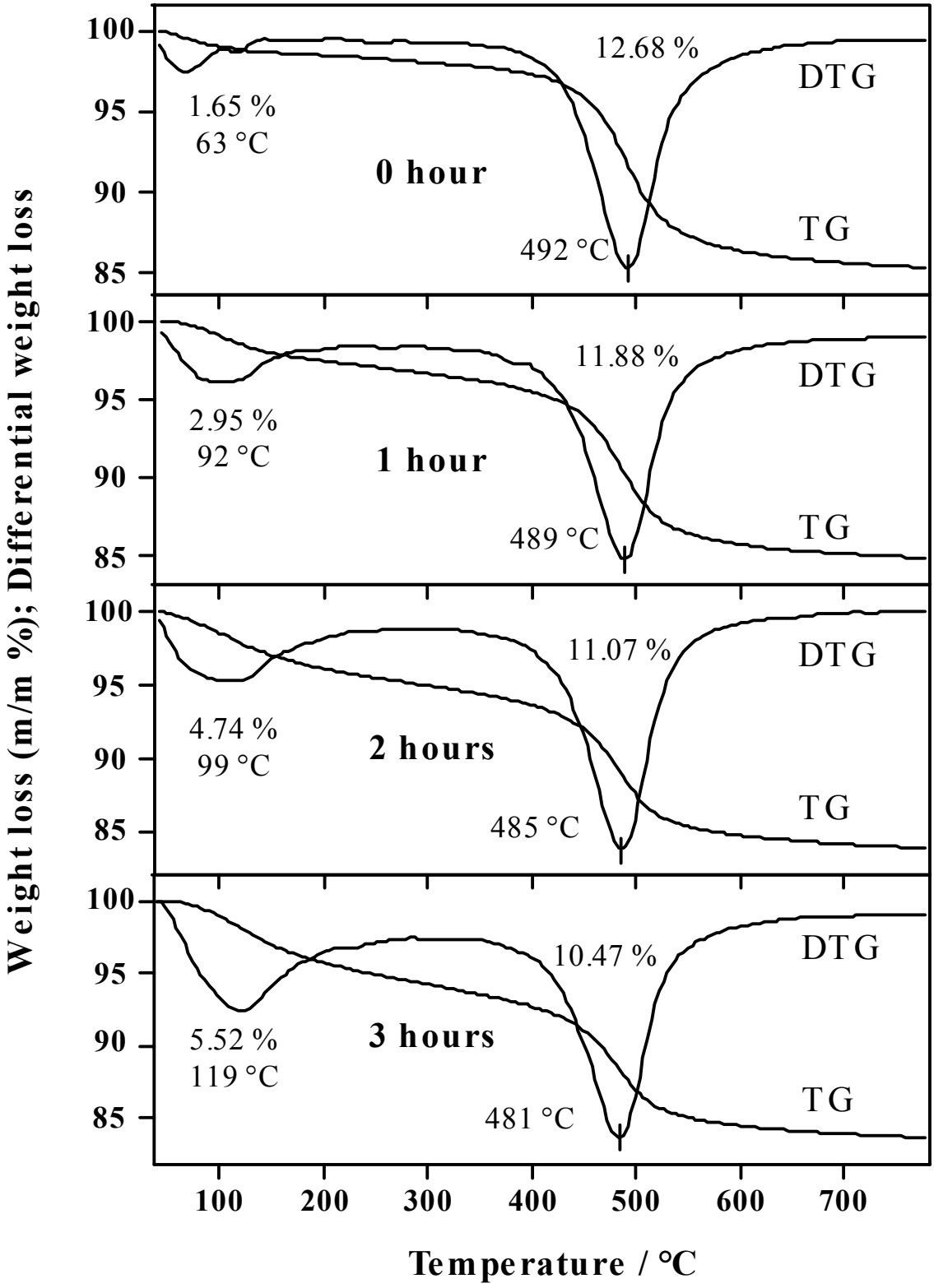

Figure 3d Frost et al.

Szeg

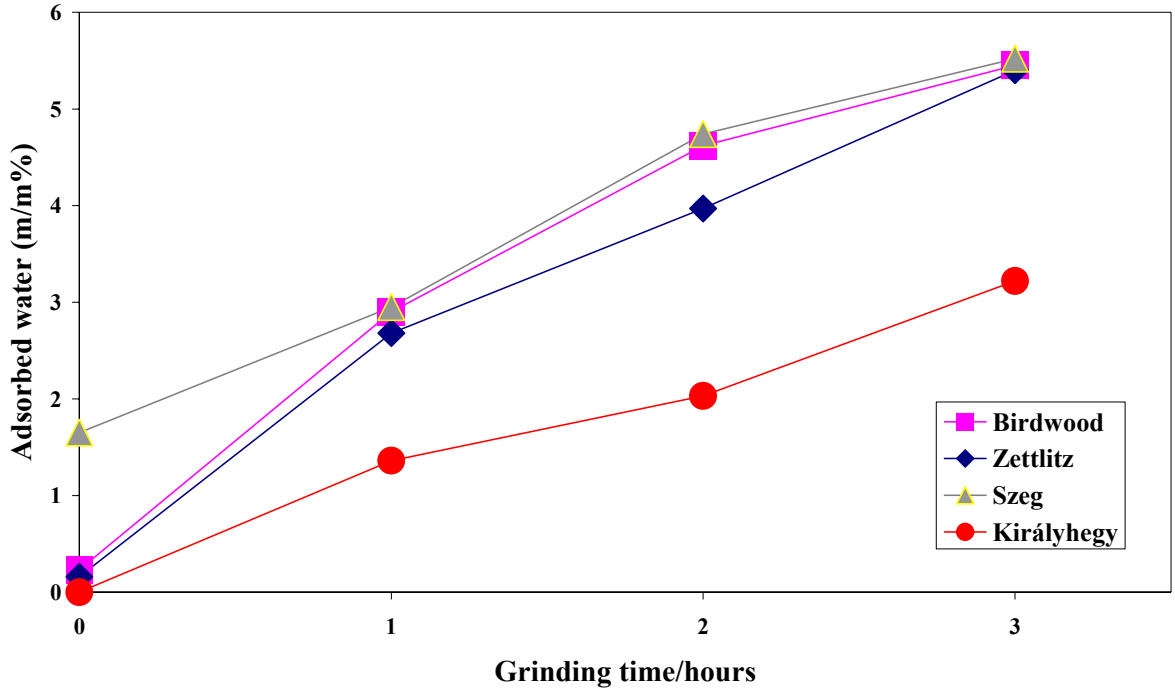

Figure 4a

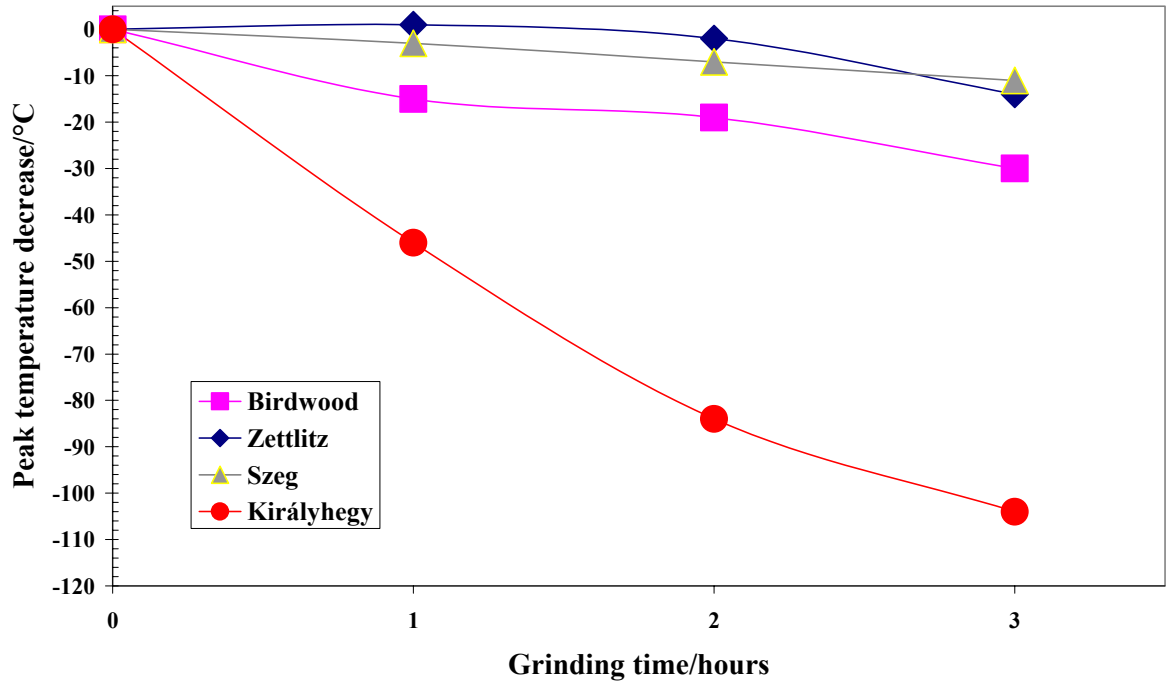

Figure 4b

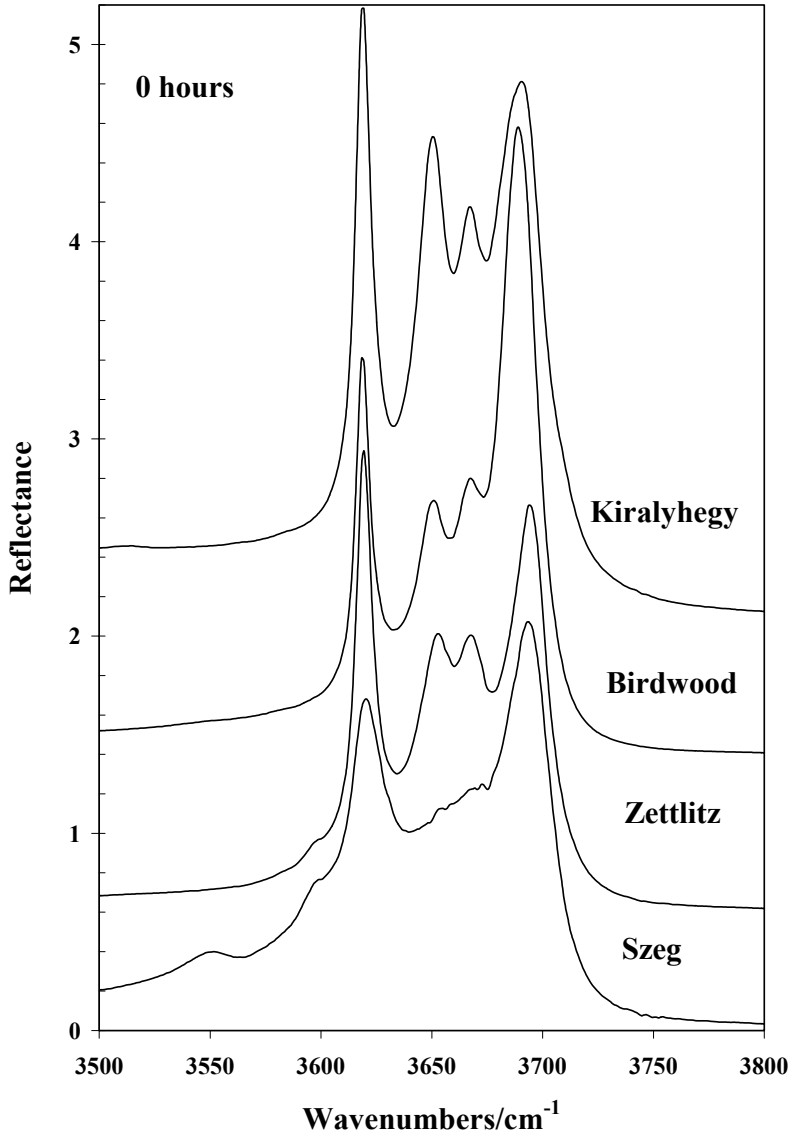
0 hours
Kiralyhegy
Birdwood
Zettlitz
Szeg
Reflectance
Wavenumbers/cm-1
0
1
2
3
4
5
3500
3550
3600
3650
3700
3750
3800

Figure 5a

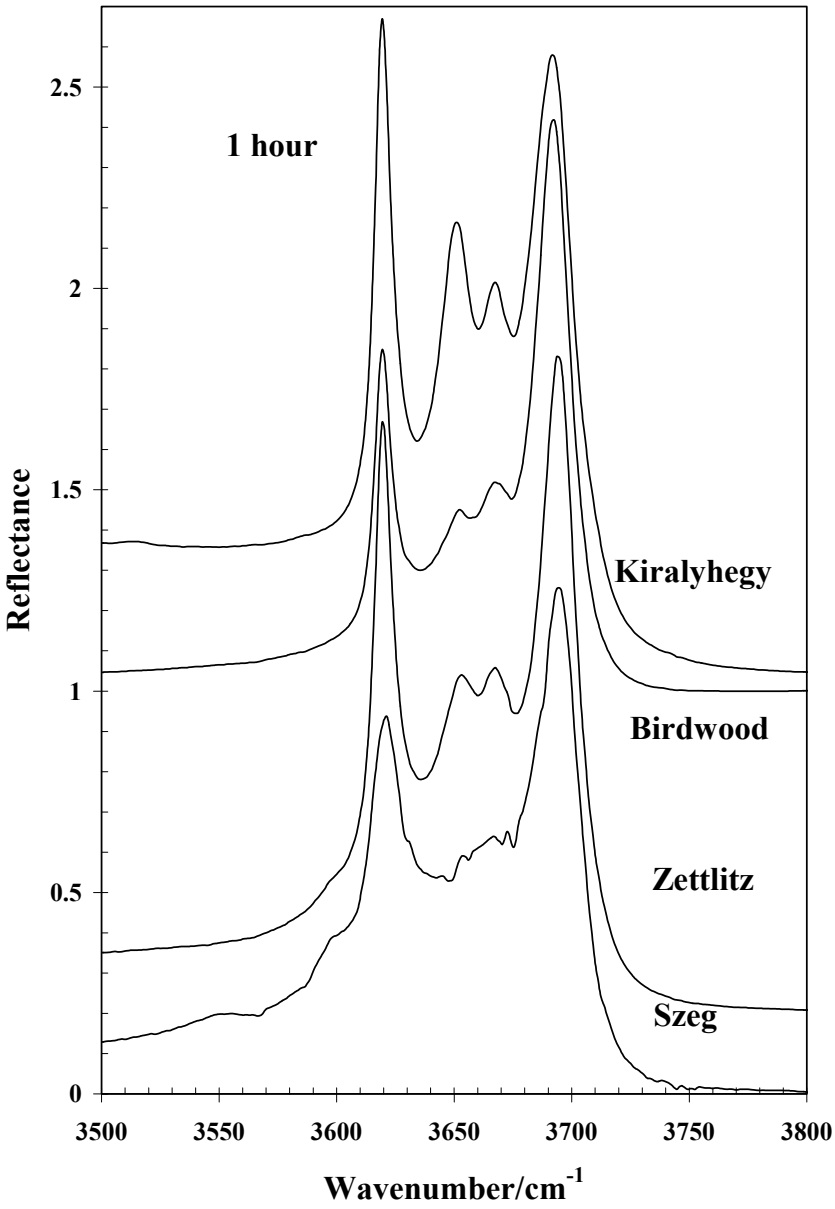
1 hour
Kiralyhegy
Birdwood
Zettlitz
Szeg
Reflectance
Wavenumber/cm-1
0
0.5
1
1.5
2
2.5
3500
3550
3600
3650
3700
3750
3800

Figure 5b

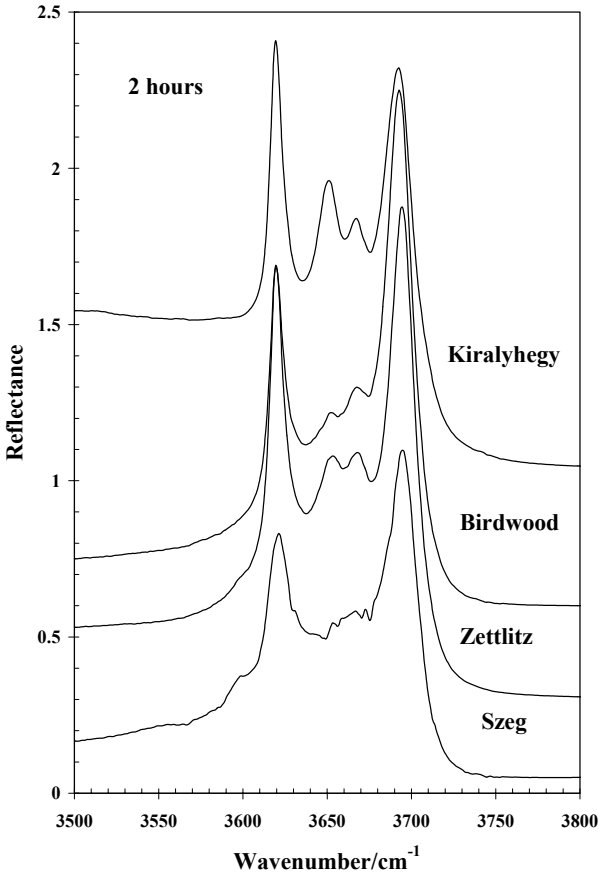
2 hours
Kiralyhegy
Birdwood
Zettlitz
Szeg
Reflectance
Wavenumber/cm-1
2.5
2
1.5
1
0.5
0
3500
3550
3600
3650
3700
3750
3800

Figure 5c

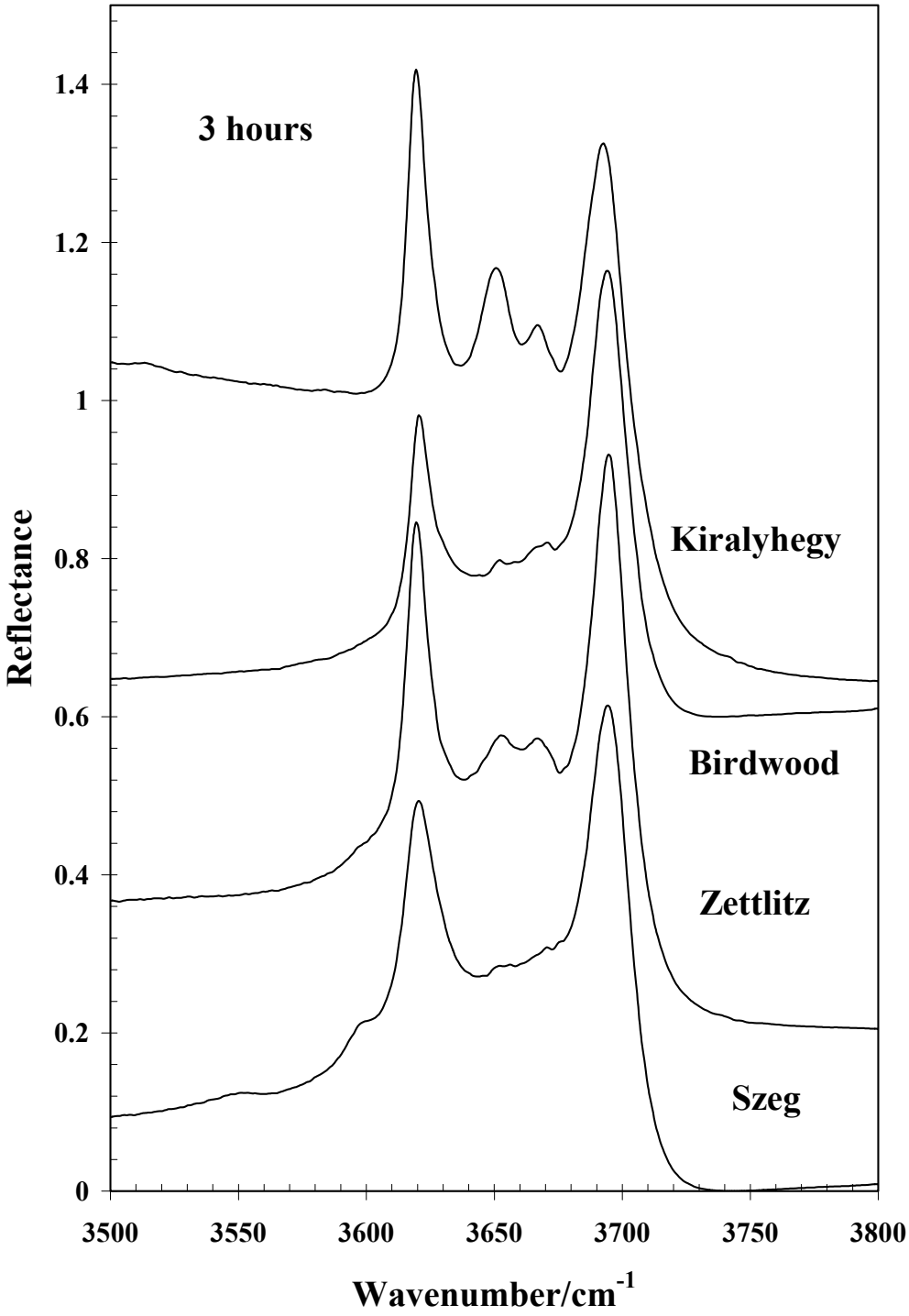
3 hours
Kiralyhegy
Birdwood
Zettlitz
Szeg
Reflectance
Wavenumber/cm-1
0
0.2
0.4
0.6
0.8
1
1.2
1.4
3500
3550
3600
3650
3700
3750
3800

Figure 5d

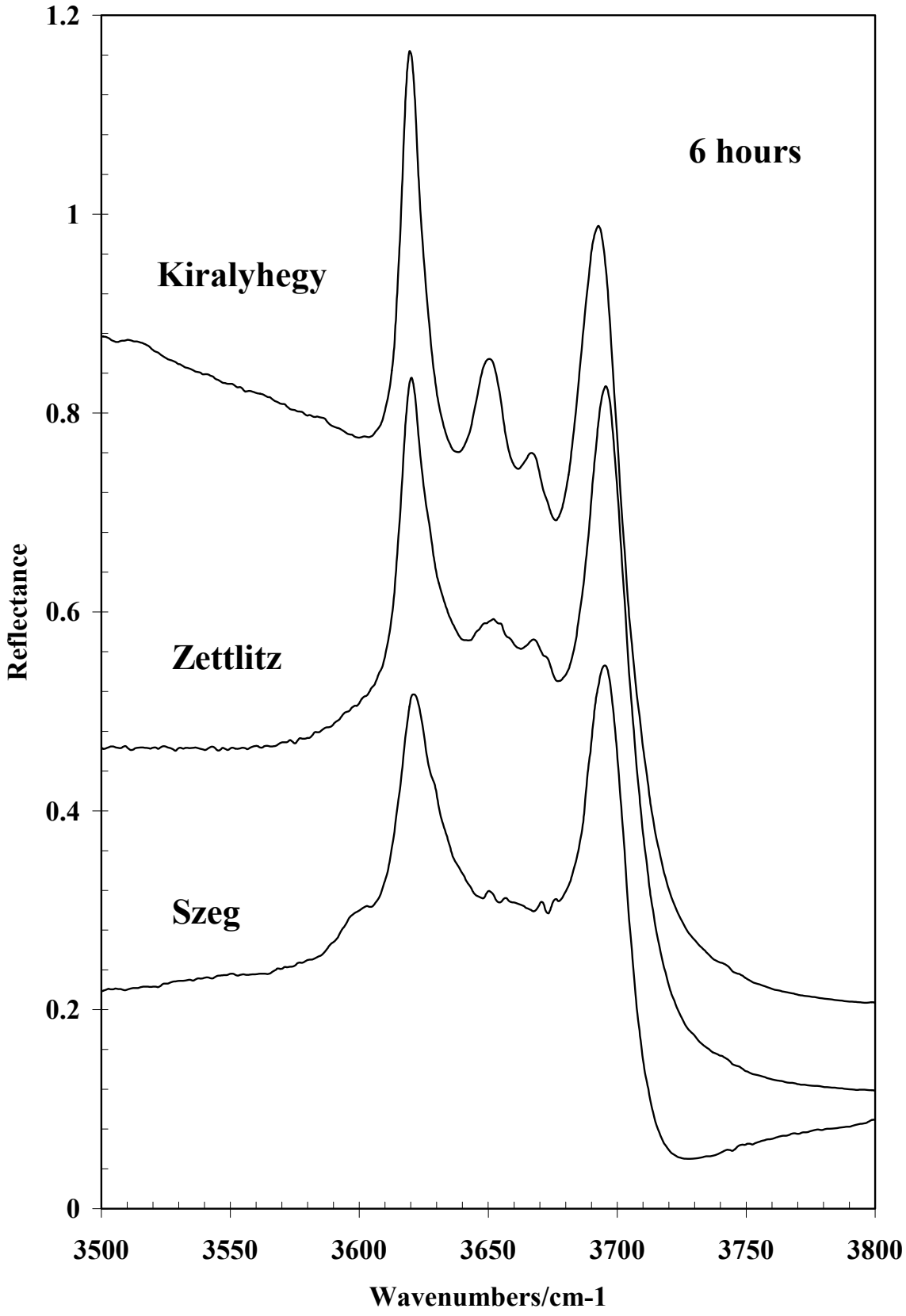
1.2
1
0.8
0.6
0.4
0.2
0
Reflectance
6 hours
Kiralyhegy
Zettlitz
Szeg
3500
3550
3600
3650
3700
3750
3800
Wavenumbers/cm-1

Figure 5e

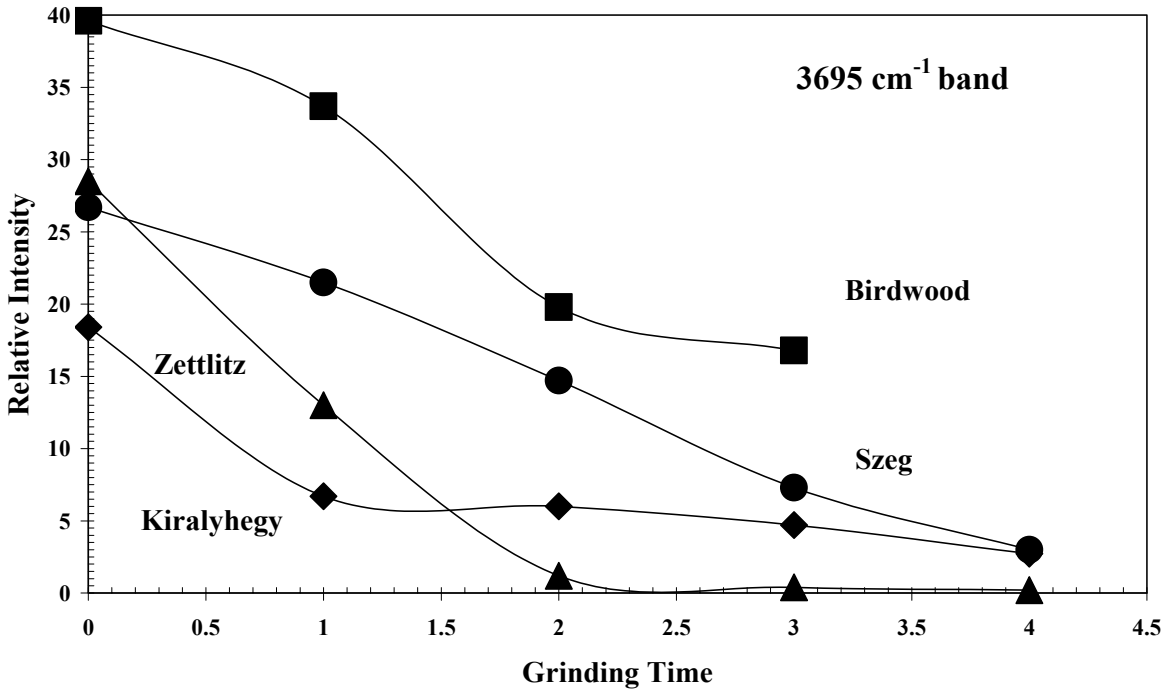
3695 cm-1 band
Birdwood
Szeg
Zettlitz
Kiralyhegy
Relative Intensity
Grinding Time
0
5
10
15
20
25
30
35
40
0
0.5
1
1.5
2
2.5
3
3.5
4
4.5

Figure 6a

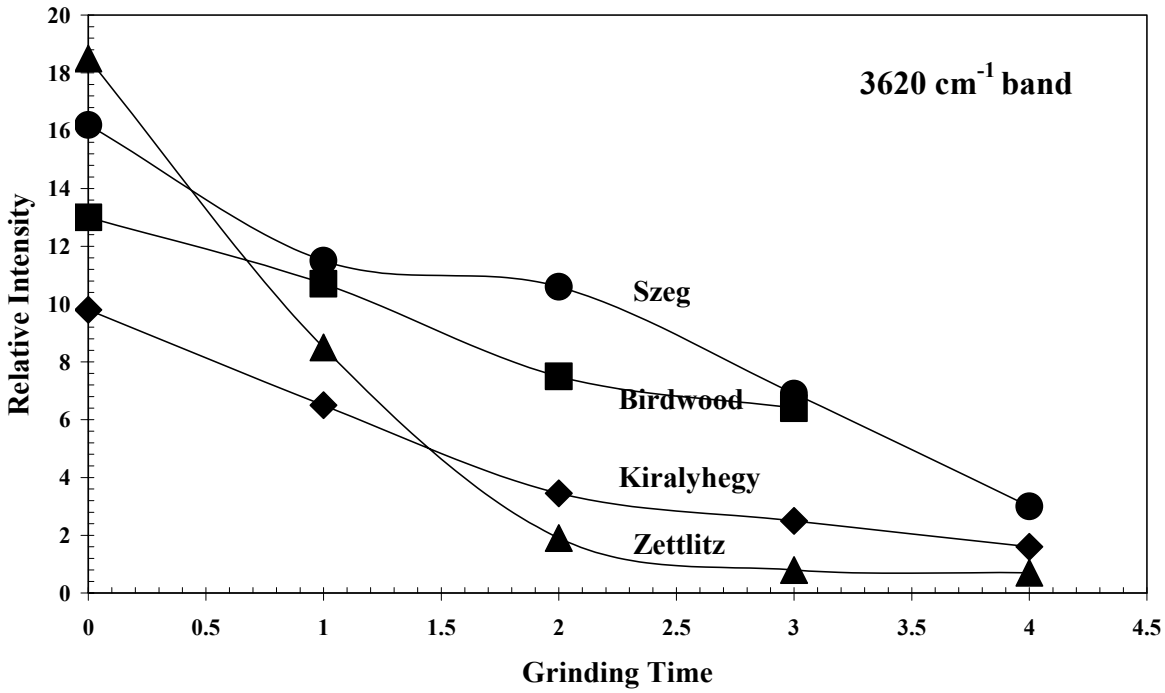
3620 cm-1 band
Relative Intensity
Grinding Time
Szeg
Birdwood
Kiralyhegy
Zettlitz
0
2
4
6
8
10
12
14
16
18
20
0
0.5
1
1.5
2
2.5
3
3.5
4
4.5

Figure 6b

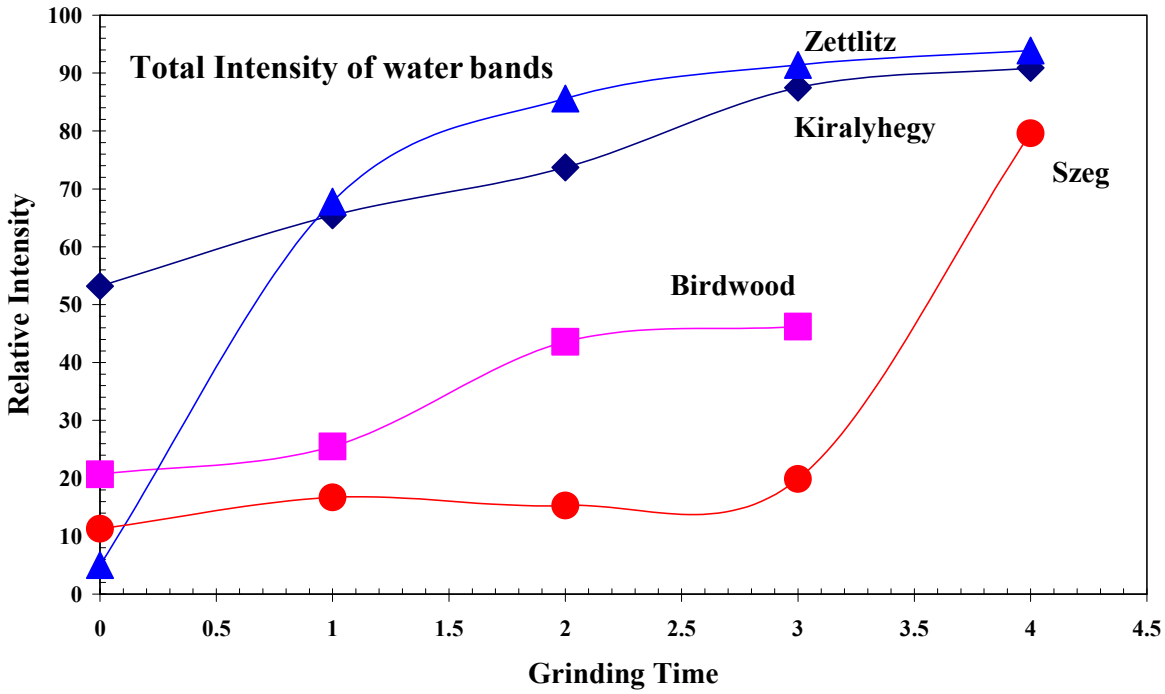
Total Intensity of water bands
Zettlitz
Kiralyhegy
Szeg
Birdwood
Relative Intensity
Grinding Time
100
90
80
70
60
50
40
30
20
10
0
0
0.5
1
1.5
2
2.5
3
3.5
4
4.5

Figure 6c

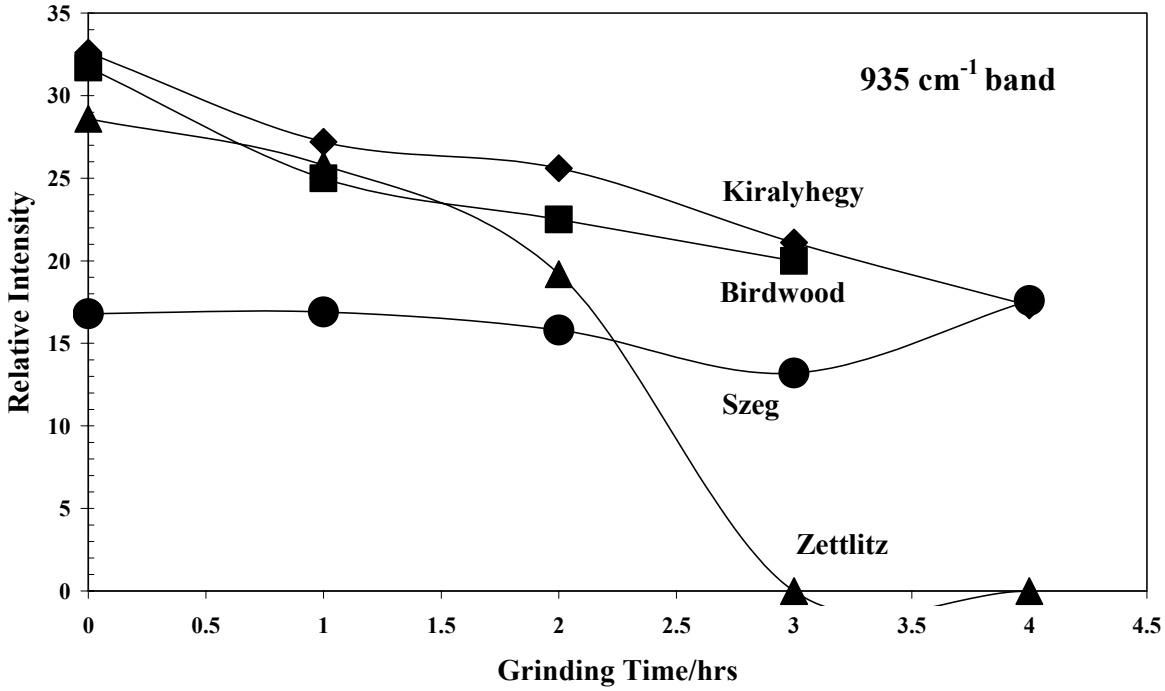
935 cm-1 band
Kiralyhegy
Birdwood
Szeg
Zettlitz
Relative Intensity
Grinding Time/hrs
0
5
10
15
20
25
30
35
0
0.5
1
1.5
2
2.5
3
3.5
4
4.5

Figure 7a

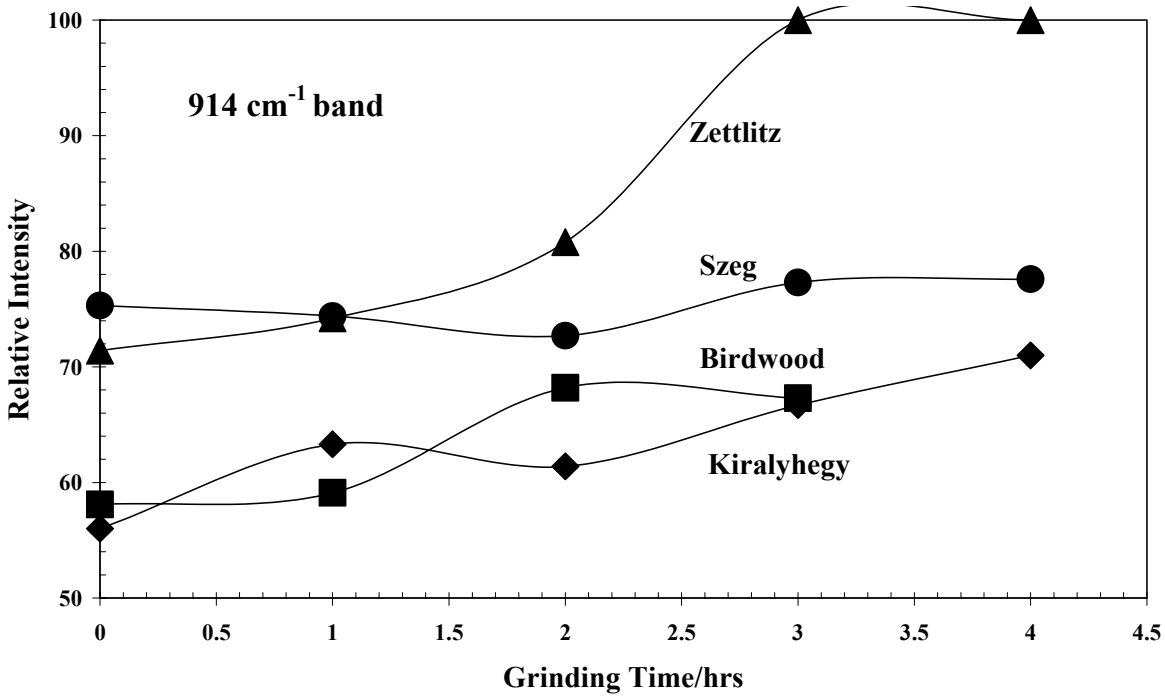
914 cm-1 band
Zettlitz
Szeg
Birdwood
Kiralyhegy
Relative Intensity
Grinding Time/hrs
100
90
80
70
60
50
0
0.5
1
1.5
2
2.5
3
3.5
4
4.5

Figure 7b